International Journal of Scientific Research in Engineering and Management (IJSREM)
Volume: 10 Issue: 10 | Oct - 2026 SJIF Rating: 8.659 ISSN: 2582-3930

Photonic Crystal Fibers: A Review of Structural Design, Tunable Devices and Sensing Applications

Geerthana S[1], Mathesh M[2], Mohamed Basith M[2], Mohammad Imthiyas T[2], Moneesh S[2]

[1]Assistant Professor, Electronics and Communication Engineering, K Ramakrishnan College of Technology, Tiruchirappalli, India
[2]Student, Electronics and Communication Engineering, K Ramakrishnan College of Technology, Tiruchirappalli, India

Abstract—Photonic crystal fibers (PCFs) have evolved in the past two decades from an experimental phenomenon to a highly versatile platform in modern photonics, mostly due to the highly flexible structural properties enabled by the microstructured air-hole cladding. This paper reviews the main research directions in PCF technology, which include the guiding principle, mode and polarization control, dispersion and nonlinear-optical effects management, liquid crystal and fluid-filled tunable devices, physical parameter sensors, biosensors and chemical sensors, terahertz photonics, and fiber-to-fiber couplers. For all research areas, the governing physical principle, representative device configurations, and performance indicators are described and compared. Comparative analysis of the reported sensitivity values of sensing devices is performed. Besides that, major problems in the field related to fabrications, stability, and integration of various applications are considered, along with new directions of research, such as hybrid PCF-metasurface biosensors, mid-infrared PCFs made of soft glass and chalcogenides, and machine learning-based approach to PCF design.

Key Words: Photonic Crystal Fiber (PCF), biosensor, Surface Plasmon Resonance (SPR), liquid crystal, dispersion compensation, orbital angular momentum, terahertz photonics, fiber optic sensor.

1. INTRODUCTION

Photonic Crystal Fibers (PCF) have gained a lot of interest among scientists due to the special features of their structure and high performance capabilities. As opposed to regular optical fibers whose structure consists of a solid core and cladding made of materials with different refractive indexes, photonic crystals feature a microstructured section with periodically arranged air holes running through the fiber. Due to the special design, the fibers provide for efficient light confinement in the core and control of important optical parameters such as dispersion, birefringence and nonlinearity, making PCFs very appropriate for modern photonic technologies [1]. The present review focuses on the major advantages of PCFs, their variety of applications, recent advances in fabrication techniques and possible prospects for further research. The special optical properties, flexibility of design and wide applications make PCFs a very interesting technology for future photonics and optical fibers.

Section 2 describes the basic guiding mechanisms and geometrical configurations of PCFs with particular focus on index guiding and photonic band-gap guiding. Section 3 covers mode and polarization engineering in PCFs with discussion of OAM modes, polarization manipulation, birefringence, and mode conversion techniques. Section 4 addresses dispersion and nonlinear-optical engineering in PCFs with regard to dispersion control, slow light phenomena, and nonlinear optics. Section 5 considers PCF-based devices with use of liquid crystals and infiltrated liquids. Section 6 describes PCF devices for measurement of physical parameters including strain, temperature, pressure, and electric field. Section 7 covers PCF-based biosensing and chemosensing technologies with particular attention to surface plasmon resonance devices and interferometric sensors. Section 8 covers the design of PCF devices suitable for terahertz frequencies. Section 9 is about interfacing PCFs with other optical fibers. Section 10 provides comparative analysis of all sensing technologies described in this review. Section 11 identifies the main problems related to the use of PCFs and discusses further research directions. Finally, Section 12 offers conclusions and summary of the review.

2. FUNDAMENTALS OF PCF GUIDANCE AND STRUCTURAL DESIGN

The earliest and most structurally distinctive class of PCFs exploits the photonic bandgap effect in hollow cores. Mangan et al. demonstrated the first hollow-core PBG fiber containing multiple independently guiding hollow cores within a single cladding, opening a path toward highly multicore hollow-core designs for parallel low-nonlinearity transmission and gas-based nonlinear optics [1]. A related but structurally distinct approach uses quasi-periodic, rather than strictly periodic, cladding lattices: Sun and Hu analyzed a twelve-fold quasi-crystalline hollow-core fiber, showing that the quasi-periodic arrangement supports two separate bandgaps and hence two low-loss spectral guidance windows, giving additional design freedom over conventional triangular-lattice PBG fibers [2].

Solid core index-guiding photonic crystal fibers (PCFs) have remained an essential basis for designing high-power laser systems and sensors due to their simple fabrication procedure. Napierała et al. fabricated a large mode area PCF, which would eliminate higher order modes in coiling condition with a bending radius of 10 cm. Such a PCF could achieve near single-mode operation in compact fiber-laser and amplifier systems with a large mode area [3]. For even more demanding conditions, Wang et al. utilized femtosecond-laser direct writing technique for fabricating photonic-crystal waveguide and fiber Bragg grating in sapphire. The obtained single-mode index guiding sapphire PCF temperature sensor was capable of operating in severe conditions close to 2000 °C, thus breaking the limitation of practical operating temperature of usual silica PCFs [5]. Another study conducted by Baghdasaryan et al. focused on investigation of graded index photonic-crystal “Mikaelian lenses,” which have been created by changing air hole diameter or pitch in the cladding region. These photonic crystals were suggested to be used as transversely focusing devices in microstructured fiber cladding in order to increase femtosecond-laser grating inscription efficiency [4].

Fig. 1 shows the structure of both solid-core and hollow-core photonic crystal fibers (PCFs). Generally, these fibers are made up of an ordered structure of air holes around the central core. Based on their structure, the guidance of light can be done by either modified total internal reflection or photonic bandgap effect.

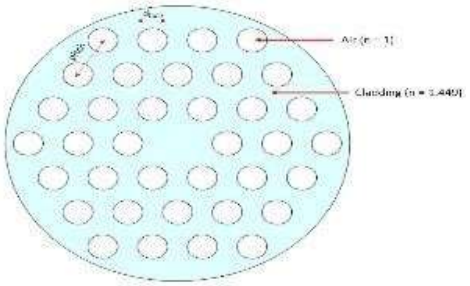


Fig. 1. Typical photonic crystal fiber structures

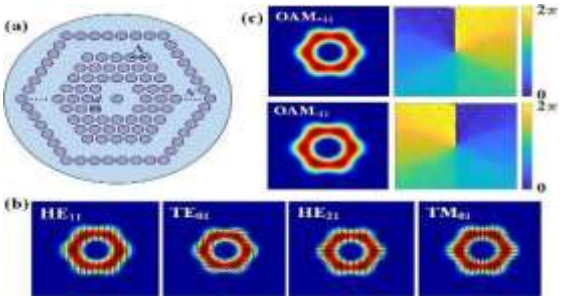


Fig. 2. Representative PCF structures for mode conversion, orbital angular momentum transmission, polarization control, and birefringence enhancement.

3. MODE AND POLARIZATION ENGINEERING

Design flexibility of PCFs' cladding lattices serves as an efficient tool to control the number of guided modes, their symmetry, and polarization. Zhang et al. have designed PCF with the circular cladding lattice pattern instead of standard hexagonal one with 14 OAM modes having low confinement losses and attaining 3.434×10^{-9} dB/m for the HE_{41} mode along with the wide common bandwidth of 560 nm. Such fiber parameters make it a good choice for use in MDM optical communication systems [6]. Cai et al. suggested dual-core PCF including both index-guiding core and PBG core; by placing high-index rods near one of them, efficient conversion of spatial modes between these two guiding principles with wavelength-tunable properties becomes possible [7]. Polarization control was also demonstrated using the combination of structure and materials engineering. The study conducted by Chen et al. utilized nematic liquid crystal to infiltrate the coupling core of a dual-core PCF to design a polarization splitter with ultra-wide operating bandwidth of 250 nm and an extinction ratio of over −20 dB for operation in the E, S, C, and L bands [8]. In a different study, Yang et al. used a square-lattice high birefringence microstructure to design a Lyot-type PCF depolarizer that could rotate polarization by 45° during propagation [9].

Birefringence and nonlinearity have also been jointly engineered at the material level. Huang et al. proposed a slot-spiral silicon PCF that numerically achieves simultaneously high birefringence and high nonlinearity, of interest for compact nonlinear silicon photonic devices [10]. Beyond steady-state mode design, Kovačević et al. studied the spatial transients of modal power distribution along multimode solid-core W-type PCFs, showing that the distance required to reach steady-state mode coupling depends on the number of cladding rings, hole size and spacing, and the launch condition - a practical consideration for any multimode PCF link or sensor whose performance depends on modal equilibrium [12]. Examples of PCFs for mode control and polarization control are illustrated in Fig. 2. The PCFs have been fabricated through the design of air-holes structure, core structure, and lattice structure; therefore, the PCFs can be fabricated to possess the orbital angular momentum modes and high birefringence.

4. DISPERSION AND NONLINEAR-OPTICAL ENGINEERING

Because the dispersion properties of photonic crystal fibers (PCFs) can be designed in significant freedom from the dispersion of the materials used, photonic crystal fibers are extensively used for dispersion compensation, slow-light generation, and soliton applications. Sinha et al. designed single mode As2Se3 chalcogenide PCF for generating tunable slow light by stimulated Brillouin scattering. Numerical analysis demonstrated that the Brillouin scattering gain coefficient was approximately 88 dB/m, while a delay of up to 137 ns was achieved using a 1 m-long PCF with a pump power of 100 mW [13]. In another study, Sivabalan and Raina proposed a photonic quasi-crystal fiber stretcher for chirped-pulse amplification systems, exhibiting a high normal group velocity dispersion of 1000 ps/(nm·km) and an effective mode area of 35 μm² [14].

For wavelength-division-multiplexing (WDM) transmission, Hsu et al. proposed a wavelength-tunable dispersion-compensating PCF combining a dual-concentric-core structure with a depressed-clad structure, in which inserting index rods of different refractive index into the central core shifts the operating wavelength while maintaining a large negative dispersion coefficient, suitable for conventional/coarse WDM systems [15]. Tee et al. demonstrated broadband dispersion compensation using a nested PCF-in-PCF configuration, in which one photonic crystal fiber was incorporated within another. The proposed structure provided a flattened average dispersion of −457.4 ps/(nm·km) over a broad wavelength range of 1360–1690 nm, covering the combined E+S+C+L+U telecommunication bands [16]. In the nonlinear regime, Yuan et al. utilized the interplay between dispersion and birefringence in a highly birefringent PCF to produce wavelength-tunable, two-color solitons through intrapulse Raman scattering. A tuning range of approximately 300 nm was obtained within the 2100–2370 nm wavelength region, demonstrating its potential for broadband mid-infrared generation [17]. As illustrated in Fig. 3, the dispersion characteristics of PCFs can be effectively controlled by modifying structural parameters such as the air-hole diameter, pitch, and core geometry. This design flexibility enables PCFs to provide tailored dispersion properties for applications such as dispersion compensation, dispersion management, and supercontinuum generation.

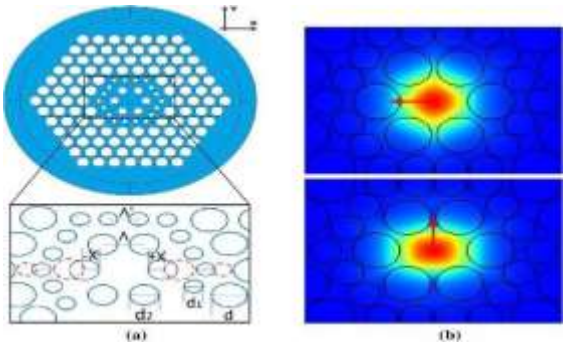


Fig. 3. Dispersion-engineered PCF designs used for nonlinear optics, supercontinuum generation and slow-light applications.

5. LIQUID-CRYSTAL AND FLUID-INFILTRATED PCF DEVICES

The selective infiltration of liquid crystal (LC) or other functional fluids into the air holes of a PCF enables the transformation of a passive waveguide into an actively controllable and environmentally sensitive platform. This design concept is reported in nine of the papers considered in this review. Mathews et al. showed that nematic-LC-infiltrated polarization-maintaining PCF exhibits direction-dependent sensitivity to an externally applied electric field, enabling two-dimensional directional electric-field sensing with a simple polarimetric read-out [18], and subsequently characterized the frequency response of such LC-infiltrated PCFs from 50 Hz to 1 kHz, finding a transmittance response at twice the applied field frequency due to the millisecond-order LC relaxation time [19]. Building on this concept with an active demodulation scheme, Liu et al. embedded an LC-filled PCF Mach–Zehnder interferometer inside a fiber ring laser, exploiting the photonic bandgap effect and ring-laser gain to more than double the electric-field sensitivity to 1.1 nm/Vrms with a 35 dB signal-to-noise ratio and long-term stability better than 0.15 nm over 2.5 hours [20].

Temperature sensing is another major use of LC infiltration. Sun et al. selectively filled a single air hole near the core of a PCF, producing three resonance dips arising from coupling between the LP_{01} core mode and LP_{03}/LP_{51} rod modes, whose shift with temperature tracks the thermo-optic behavior of the LC and enables compact temperature measurement [21]. Milenko et al. compared PCF and Photonic Liquid-Crystal Fiber (PLCF) modal interferometers experimentally, showing that infiltrating the PCF with LC and heating the resulting PLCF interferometer provides a tunable, temperature-responsive optical characteristic distinct from the unfilled PCF [22]. At larger mode-field scales, Tefelska et al. demonstrated large-area multimode PBG propagation in a 50 µm core LC-filled PCF, achieving what was, at the time, the lowest reported attenuation (0.16 dB/cm) for such a fiber, aided by reduced overlap between the guided mode and the LC-filled holes [23]. Material-level tunability was pushed further by Hameed et al., who combined a soft-glass PCF cladding with a nematic-LC-filled core to obtain simultaneously high birefringence (0.042) and high nonlinearity for both quasi-TE and quasi-TM modes [11]. Non-LC fluids have also been used for thermo-optic control: Wang et al. showed that filling the air holes of a solid-core PCF with an absorbing fluid produces a thermo-optically switchable transmission with a 30 dB extinction ratio for only a 10 °C temperature change [24], and Hossain and Faisal theoretically analyzed a chloroform-filled chalcogenide PCF Sagnac interferometer for mid-infrared temperature sensing, reporting sensitivities of −5.77 nm/°C and 8.49 nm/°C for two resonance dips with full infiltration [25]. The structure of typical liquid crystal and fluid infiltrated PCFs is shown in Fig. 4. Functional materials selectively injected into air holes change the effective refractive index, leading to electric and thermal tuning ability of sensors.

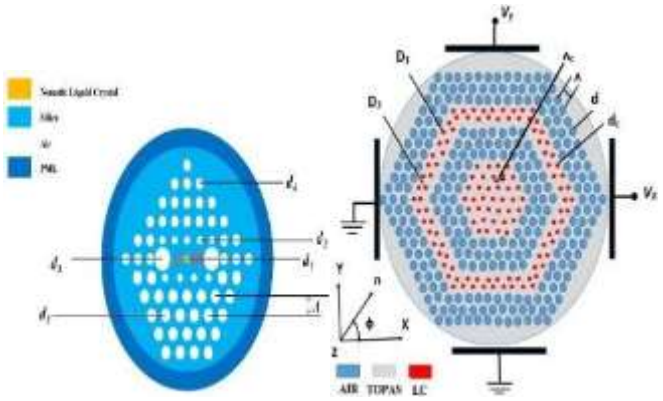


Fig. 4. Liquid-crystal and fluid-filled photonic crystal fibers illustrating selective infiltration of air holes for tunable sensing applications.

6. PCF-BASED PHYSICAL-PARAMETER SENSORS

In addition to fluid infiltration techniques, PCFs are extensively integrated with interferometric and grating-based detection methods for the measurement of parameters such as strain, pressure, and temperature. Rajan et al. integrated a polarimetric PCF sensor with a Fiber Bragg Grating (FBG) sensor, enabling polarization and wavelength information to be transformed into a common intensity-based output. This configuration allowed simultaneous discrimination of strain and temperature, which could not be achieved using either sensor independently [26]. For dedicated strain measurement, Gong et al. constructed a Sagnac loop using a 140 mm-long section of low-birefringence PCF. The sensor exhibited a strain sensitivity of 0.457 pm/µε across a strain range of 0–2520 µε, while its corresponding temperature cross-sensitivity was also investigated [27]. In the area of pressure sensing, Hu and Chen introduced a side-hole dual-core PCF, where two relatively large air holes positioned outside the photonic-crystal region function as integrated pressure-sensitive elements. These structural features increase the pressure-induced refractive-index variation and consequently enhance inter-core mode coupling, providing the operating principle for hydrostatic pressure detection [28]. Most recently, Shi et al. combined a gold-coated surface-plasmon-resonance (SPR) channel with a toluene-filled directionally coupled channel in the same dual-channel PCF to simultaneously monitor DNA concentration and temperature while minimizing the cross-influence of temperature on the biosensing channel [29]. Fig. 5 depicts a few PCF physical sensors. Changes in strain, temperature, pressure, and electrical field cause variations in the optical characteristics of the guided mode, enabling precise measurements using interferometric or grating techniques.

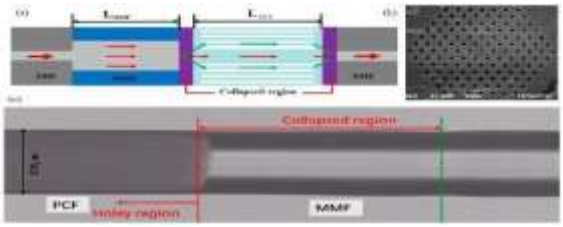


Fig. 5. Representative PCF-based sensors for measuring strain, temperature, pressure, and electric fields.

7. PCF-BASED BIOSENSORS AND CHEMICAL SENSORS

Rifat et al. developed a two-ring hexagonal-lattice SPR-PCF biosensor in which the gold layer and analyte were positioned externally rather than within the fiber's air holes. This configuration simplifies the overall fabrication process while maintaining the functionality of the biosensing structure. The sensitivity achieved in wavelength is 4000 nm/RIU, while that in amplitude is 320 RIU^{-1} [30]. Interferometric techniques do not involve the use of metallic layers. In the work by Hu et al., a small piece of PCF with the length of 3 mm was used between two single-mode fibers, whereby the collapsed-void microbubble region excited cladding modes. This setup helped realize PCF modal-interferometric bioaffinity sensing based on streptavidin–biotin interaction, resulting in sensitivity of 320 nm/RIU [31]. Further development of this technique was made by Deng et al., who introduced a spherical reflector at the end facet of the endlessly single-mode PCF core-cladding-mode interferometer, achieving the sensitivity of about 199 nm/RIU and enhancing the compactness and stability [32]. For selective molecular detection, Coscelli et al. modified the inner surface of a suspended-core PCF by incorporating peptide nucleic acid (PNA) probes, enabling specific interaction with the target molecules.

Numerical investigations of SPR-PCF configurations have also focused on the selective detection of pathogenic microorganisms. Haque et al. proposed a gold-coated square-lattice photonic crystal fiber SPR biosensor for detecting waterborne pathogens, including *Vibrio cholerae*, *E. coli*, *Bacillus anthracis*, and *Enterococcus faecalis*. Among the microorganisms investigated, the sensor exhibited a maximum wavelength sensitivity of 5161 nm/RIU for *E. faecalis* [34]. Jahan et al. developed a gold-coated circular-lattice PCF SPR biosensor for *Pseudomonas* detection. The proposed sensor achieved a wavelength sensitivity of 20,000 nm/RIU and an amplitude sensitivity of 1380 RIU^{-1}, with a spectral resolution of 5.26×10^{-6} RIU over a refractive-index range of 1.33–1.42 RIU [35]. Mohammed et al. reviewed various photonic-crystal and photonic-crystal-fiber-based on-chip biomedical sensors, comparing key performance characteristics such as sensitivity, quality factor, and device compactness. Their study also discussed potential directions for the development of next-generation photonic-crystal biomedical sensing platforms [36]. Fig. 6 presents the schematic representation of an SPR-based PCF biosensor, in which high sensing performance is obtained through the interaction and coupling between the guided optical mode and the adjacent metal plasmonic layer.

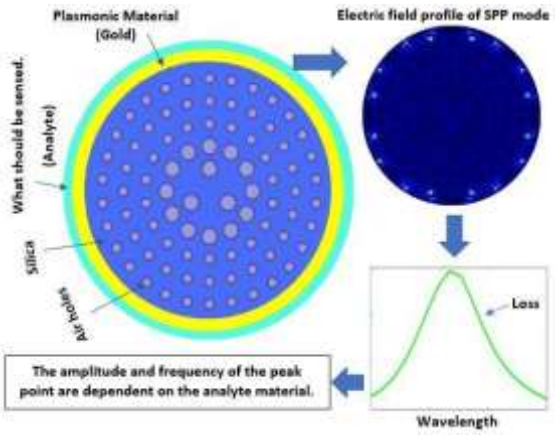


Fig. 6. Surface plasmon resonance (SPR)-based photonic crystal fiber biosensor with an external gold layer for high-sensitivity refractive-index sensing.

8. TERAHERTZ-REGIME PCF DEVICES

Furthermore, the microstructuring concepts employed in near-infrared photonic crystal fiber (PCF) designs can be extended to the terahertz (THz) frequency regime, particularly through the use of polymer-based structures and porous-core fibers. Stecher et al. fabricated two-dimensional polymeric photonic-crystal band-stop filters operating in the THz region using the conventional fiber-drawing technique. The frequency- and angle-dependent characteristics of the fabricated structures were subsequently investigated using THz time-domain spectroscopy [37]. For the detection of different blood constituents, including red blood cells, hemoglobin, white blood cells, plasma, and water, in the THz frequency range, Ahmed et al. proposed a partially structured type-B crystalline-core PCF operating between 1.5 and 3.5 THz. The proposed fiber achieved a sensitivity of 80.93% at 1.5 THz, while maintaining a relatively low confinement loss, indicating its potential for THz-based biomedical sensing applications [38]. It is seen from Fig. 7 that porous-core configuration decreases material absorption and gives good mode confinement for this type of photonic-crystal fiber.

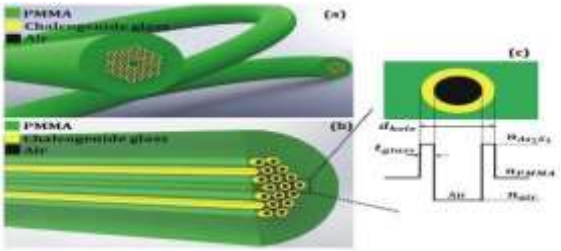


Fig. 7. THz photonic crystal fiber design with porous and polymer core materials for efficient THz wave transmission.

9. FIBER INTERFACING: COUPLING AND SPLICING

Unlike conventional single-mode fibers, PCFs generally exhibit small and distinctive mode-field profiles, making efficient fiber interfacing a critical consideration in their practical implementation. Ouyang et al. addressed the mode-field mismatch between a double-clad fiber and a PCF by introducing a graded-index fiber (GIF) lens and a coreless fiber section between the two fibers. This approach minimized the splicing loss between fibers having mode-field diameters of 18.7 µm and 3.9 µm, respectively, achieving a loss as low as 0.5 dB after optimizing the lengths of the GIF and coreless fiber [39].

In contrast, Wei et al. numerically investigated an evanescent-field side-polished coupler designed to connect a single-mode fiber with a PCF. Their proposed configuration achieved a maximum coupling ratio of 93% with a coupling length of 1.72 mm. The study also highlighted the need to consider both insertion loss and propagation attenuation during coupler design, parameters that had been overlooked in several earlier studies of evanescent-field couplers [40]. Fig. 8 illustrates the coupling and splicing arrangement between a conventional single-mode fiber and a photonic crystal fiber.

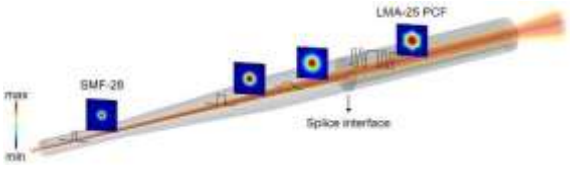


Fig. 8. Coupling and splicing techniques between conventional optical fibers and photonic crystal fibers using graded-index lenses and fusion splicing.

10. COMPARATIVE DISCUSSION

Table 1 consolidates the reported sensitivities and key performance figures across the sensing-oriented studies reviewed in Sections 5–7. Two broad trends emerge. First, SPR-based PCF biosensors that place the metal layer and analyte externally consistently report the highest wavelength sensitivities, in the multi-thousand nm/RIU values due to the flexibility in optimizing the plasmonic layer thickness and the lattice structure without facing difficulties involved in selective deposition of metals onto internal air hole walls. Second, interferometric and Sagnac-loop-type sensors usually have relatively lower sensitivities, namely between tens and hundreds of nm/RIU or pm per microstrain/°C, but they benefit from an easier fabrication process based on fusion splicing rather than metal coating and also self-referencing. This justifies their usage for applications in strain and bulk RI sensing, where reliability and reproducibility can outweigh the highest achievable sensitivity. The same tradeoff is observed in the LC and fluid-filled devices considered in section 5: infiltration can drastically increase the sensitivity to electrical field and temperature, but can create additional problems concerning stability, length of the filling region, and response speed determined by relaxation time of the filling material.

An important point is that the choice of the sensing mechanism depends mostly on the application, rather than on the sensing mechanism itself. In particular, structural health monitoring, industrial process control, and environmental sensing prefer interferometric or Sagnac-loop designs due to mechanical robustness, low manufacturing costs, and high insensitivity to external environmental influences. Likewise, liquid-crystal-infiltrated PCF sensors offer significant potential for electric-field and temperature measurements because of the strong electro-optic and thermo-optic responses of liquid crystals. However, their practical implementation requires careful consideration of factors such as thermal drift, liquid-crystal evaporation, and degradation of the sensing material, which may affect long-term sensor stability and performance. Furthermore, integrating PCF-based sensing systems with advanced signal-processing methods and artificial intelligence techniques could further improve their sensing accuracy, reliability, and overall performance. In addition, the design of efficient and cheap manufacturing procedures for PCF-based sensors. Hybrid sensors that employ different transduction methods are becoming increasingly popular among researchers.

Table 1: Reported sensitivities and key performance figures of the PCF devices reviewed in Sections 5–7 and 9

Ref	Sensor Type	Sensing Mechanism	Best Reported Sensitivity
[18]	Electric field (directional)	LC-infiltrated PM-PCF, polarimetry	Direction-dependent (qualitative)
[20]	Electric field	LC-filled PCF MZI + fiber ring laser	1.1 nm/Vrms, 35 dB SNR
[21]	Temperature	Selectively LC-filled PCF, 3 resonance dips	Dip shift tracks LC thermo-optic coeff.
[25]	Temperature (mid-IR)	Chloroform-filled PCF Sagnac loop	8.49 nm/°C / −5.77 nm/°C
[27]	Strain	Low-birefringence PCF Sagnac loop	0.457 pm/με (0–2520 με)
[28]	Hydrostatic pressure	Side-hole dual-core PCF, mode coupling	Enhanced via built-in transducer
[30]	Refractive index (SPR)	External gold layer, 2-ring PCF	4000 nm/RIU; 320 RIU^{-1}
[31]	Biomolecular	Collapsed-void modal interferometer	320 nm/RIU (bulk RI)
[32]	Refractive index	Core-cladding modal interferometer	≈199 nm/RIU
[34]	Waterborne bacteria (SPR)	Gold-coated square-lattice PCF	5161 nm/RIU (*E. faecalis*)
[35]	Pseudomonas bacteria (SPR)	Gold-coated circular-lattice PCF	20,000 nm/RIU; 1380 RIU^{-1}
[38]	Blood components (THz)	Partial type-B crystalline-core PCF	80.93% relative sensitivity
[39]	Fiber-to-fiber splicing loss	GIF + coreless fiber lens	0.5 dB splice loss
[40]	Fiber-to-fiber coupling	Evanescent side-polished coupler	93% coupling ratio

11. CHALLENGES AND FUTURE RESEARCH DIRECTIONS

A number of obstacles exist in most of the applications covered in this survey. Fabrication tolerance is one of these obstacles, as the structures mentioned such as the OAM C-PCF [6], PCF-in-PCF dispersion compensator [16], and SPR biosensors [30], [34], [35] have been largely simulated in order to investigate their properties. The performance of these structures can be highly sensitive to even minor variations of a few percent in the air-hole dimensions and spacing, making it particularly challenging to fabricate the proposed designs within the required tolerances of the fiber-drawing process. Long-term stability is another obstacle, especially for devices incorporating liquid crystals and fluids. Thermal cycling, liquid crystal degradation, fluid evaporation, and leakage can all contribute to the reduction of advantages of the devices described in Section 5. Interfacing efficiency is yet another obstacle that has been discussed in Section 9.

Future research directions worth pursuing include, firstly, hybrid PCFs consisting of a combination of plasmonic coating and liquid/gas infiltration, or two-core mode converter and surface plasmon resonance-based biosensor which may offer high sensitivity characteristic of external SPR configuration

along with multiplexing potential of dual channel configurations such as the one presented in [29]. Secondly, there will be a rise in the number of publications dealing with soft glass and chalcogenide PCFs similar to the work presented in [13], [11], and [25] due to the limitation of the spectral transparency range of silica. Lastly, because most of the PCF sensor configurations need to undergo numerical optimization through large parameter spaces, machine-learning-enabled inverse design is highly likely to be an effective strategy going forward.

12. CONCLUSION

This review has considered the studies involving the use of PCFs in applications related to their structural, dispersive, tunable, and sensing properties. While the devices considered in this review pursue different goals, from the delivery of an orbital angular momentum mode to the sensing of blood components via terahertz radiation, they all employ the same basic design parameter of PCFs, which is the size, arrangement, and filling of the microstructure air holes in the PCF. Basic guidance principles include index guidance and photonic band gap guidance, while the liquid crystals or fluids infiltration adds tunability to PCFs. Finally, the interferometric, Sagnac-loop, and surface plasmon resonance effects turn the modifications of the fiber or its environment into an optical signal. Based on the comparative study in Section 10 and the difficulties outlined in Section 11, future development of the field can be expected in both novel guidance schemes and integration of known approaches, such as plasmonics, fluids infiltration, and multicore modes engineering.

REFERENCES

1. B. J. Mangan, A. C. Muir, and J. C. Knight, “Photonic bandgap fiber with multiple hollow cores,” J. Lightwave Technol., vol. 28, no. 9, pp. 1287–1290, May 2010.
2. X. Sun and D. J. J. Hu, “Air guiding with photonic quasi-crystal fiber,” IEEE Photon. Technol. Lett., vol. 22, no. 9, pp. 607–609, May 2010.
3. M. Napierała, E. Bereś-Pawlik, T. Nasilowski, P. Mergo, F. Berghmans, and H. Thienpont, “Photonic crystal fiber with large mode area and characteristic bending properties,” IEEE Photon. Technol. Lett., vol. 24, no. 16, pp. 1409–1411, Aug. 2012.
4. T. Baghdasaryan, T. Geernaert, H. Thienpont, and F. Berghmans, “Photonic crystal Mikaelian lenses and their potential use as transverse focusing elements in microstructured fibers,” IEEE Photonics J., vol. 5, no. 4, Aug. 2013, Art. no. 2201115.
5. M. Wang, T. Liu, Z. Song, R. Reeves, F. P. Payne, I. N. Dyson, K. Zhang, T. Wang, et al., “Sapphire photonic crystal fiber sensor,” J. Lightwave Technol., early access, 2026.
6. H. Zhang, W. Zhang, L. Xi, X. Tang, X. Zhang, and X. Zhang, “A new type circular photonic crystal fiber for orbital angular momentum mode transmission,” IEEE Photon. Technol. Lett., vol. 28, no. 13, pp. 1426–1429, Jul. 2016.
7. S. Cai, S. Yu, Y. Wang, M. Lan, L. Gao, and W. Gu, “Hybrid dual-core photonic crystal fiber for spatial mode conversion,” IEEE Photon. Technol. Lett., vol. 28, no. 3, pp. 339–342, Feb. 2016.
8. H. L. Chen, S. G. Li, Z. K. Fan, G. W. An, J. S. Li, and Y. Han, “A novel polarization splitter based on dual-core photonic crystal fiber with a liquid crystal modulation core,” IEEE Photonics J., vol. 6, no. 4, Aug. 2014, Art. no. 6800110.
9. Zhe Yang, Xuan She, Chen-Ge Wang, Kan Chen, Xin-Fan Chen, and Xiao-Wu Shu, “A type of Lyot fiber depolarizer based on photonic crystal fiber,” IEEE Photon. Technol. Lett., vol. 30, no. 7, pp. 642–645, Apr. 2018.
10. T. Huang, J. Liao, S. Fu, M. Tang, P. Shum, and D. Liu, “Slot spiral silicon photonic crystal fiber with property of both high birefringence and high nonlinearity,” IEEE Photonics J., vol. 6, no. 3, Jun. 2014, Art. no. 6600607.
11. M. F. O. Hameed, S. S. A. Obayya, and H. A. El-Mikati, “Highly nonlinear birefringent soft glass photonic crystal fiber with liquid crystal core,” IEEE Photon. Technol. Lett., vol. 23, no. 20, pp. 1478–1480, Oct. 2011.
12. M. S. Kovačević, L. Kuzmanović, A. Simović, S. Savović, and A. Djordjevich, “Transients of modal-power distribution in multimode solid-core W-type photonic crystal fibers,” J. Lightwave Technol., vol. 35, no. 20, pp. 4352–4357, Oct. 2017.
13. R. K. Sinha, A. Kumar, and T. S. Saini, “Analysis and design of single-mode As_2Se_3-chalcogenide photonic crystal fiber for generation of slow light with tunable features,” IEEE J. Sel. Topics Quantum Electron., vol. 22, no. 2, Mar./Apr. 2016, Art. no. 4900706.
14. S. Sivabalan and J. P. Raina, “High normal dispersion and large mode area photonic quasi-crystal fiber stretcher,” IEEE Photon. Technol. Lett., vol. 23, no. 16, pp. 1139–1141, Aug. 2011.
15. J.-M. Hsu, C.-W. Yao, and J.-Z. Chen, “Wavelength-tunable dispersion compensating photonic crystal fibers suitable for conventional/coarse wavelength division multiplexing systems,” J. Lightwave Technol., vol. 33, no. 11, pp. 2240–2246, Jun. 2015.
16. D. C. Tee, M. H. Abu Bakar, N. Tamchek, and F. R. Mahamd Adikan, “Photonic crystal fiber in photonic crystal fiber for residual dispersion compensation over E+S+C+L+U wavelength bands,” IEEE Photonics J., vol. 5, no. 3, Jun. 2013, Art. no. 7200214.
17. J. Yuan, X. Sang, C. Yu, K. Wang, B. Yan, X. Shen, et al., “Widely wavelength-tunable two-colored solitons and small spectral component for broadband mid-infrared wavelength generation in a highly birefringent photonic crystal fiber,” IEEE Photon. Technol. Lett., vol. 24, no. 8, pp. 670–672, Apr. 2012.
18. S. Mathews, G. Farrell, and Y. Semenova, “Directional electric field sensitivity of a liquid crystal infiltrated photonic crystal fiber,” IEEE Photon. Technol. Lett., vol. 23, no. 7, pp. 408–410, Apr. 2011.
19. S. Mathews, G. Farrell, and Y. Semenova, “Experimental study on the frequency dependence of the liquid crystal infiltrated photonic crystal fibers,” IEEE Sensors J., vol. 12, no. 5, pp. 1018–1024, May 2012.
20. Y. Liu, W. Lin, M. I. Vai, P. P. Shum, L.-Y. Shao, W. He, S. Liu, F. Zhao, W. Wang, and Y. Liu, “Fiber optic electric field intensity sensor based on liquid crystal-filled photonic crystal fiber incorporated ring laser,” IEEE Photonics J., vol. 14, no. 1, Feb. 2022, Art. no. 6808305.
21. B. Sun, Z. Zhang, W. Wei, C. Wang, C. Liao, L. Zhang, and Y. Wang, “Unique temperature dependence of selectively liquid-crystal-filled photonic crystal fibers,” IEEE Photon. Technol. Lett., vol. 28, no. 12, pp. 1282–1285, Jun. 2016.
22. K. Milenko, T. R. Wolinski, P. P. Shum, and D. J. J. Hu, “Temperature-sensitive photonic liquid crystal fiber modal interferometer,” IEEE Photonics J., vol. 4, no. 5, pp. 1615–1620, Oct. 2012.
23. M. M. Tefelska, S. Ertman, T. R. Wolinski, P. Mergo, and R. Dabrowski, “Large area multimode photonic band-gap propagation in photonic liquid-crystal fiber,” IEEE Photon. Technol. Lett., vol. 24, no. 8, pp. 631–633, Apr. 2012.
24. Y. Wang, H. Bartelt, W. Ecke, K. Moerl, H. Lehmann, K. Schroeder, R. Willsch, J. Kobelke, M. Rothhardt, R. Spittel, L. Shan, S. Brueckner, W. Jin, X. Tan, and L. Jin, “Thermo-optic switching effect based on fluid-filled photonic crystal fiber,” IEEE Photon. Technol. Lett., vol. 22, no. 3, pp. 164–166, Feb. 2010.
25. M. S. Hossain and M. Faisal, “Theoretical investigation of mid infrared temperature sensor based on Sagnac interferometer using chloroform filled photonic crystal fiber,” IEEE Sensors J., vol. 21, no. 21, pp. 24157–24164, Nov. 2021.
26. G. Rajan, M. Ramakrishnan, Y. Semenova, K. Milenko, P. Lesiak, A. W. Domanski, T. R. Wolinski, and G. Farrell, “A photonic crystal fiber and fiber Bragg grating-based hybrid fiber-optic sensor system,” IEEE Sensors J., vol. 12, no. 1, pp. 39–43, Jan. 2012.
27. H. Gong, C. C. Chan, L. Chen, and X. Dong, “Strain sensor realized by using low-birefringence photonic-crystal-fiber-based Sagnac loop,” IEEE Photon. Technol. Lett., vol. 22, no. 16, pp. 1238–1240, Aug. 2010.
28. G. Hu and D. Chen, “Side-hole dual-core photonic crystal fiber for hydrostatic pressure sensing,” J. Lightwave Technol., vol. 30, no. 14, pp. 2382–2387, Jul. 2012.
29. W. Shi, X. Cheng, Y. Fan, and Y. Gu, “Externally coated dual-channel photonic crystal fiber for bio-temperature sensing,” IEEE Photon. Technol. Lett., vol. 36, no. 24, pp. 1493–1496, Dec. 2024.
30. A. A. Rifat, G. Amouzad Mahdiraji, Y. M. Sua, Y. G. Shee, R. Ahmed, D. M. Chow, and F. R. Mahamd Adikan, “Surface plasmon resonance

photonic crystal fiber biosensor: A practical sensing approach," IEEE Photon. Technol. Lett., vol. 27, no. 15, pp. 1628–1631, Aug. 2015.

31. D. J. J. Hu, J. L. Lim, M. K. Park, L. T.-H. Kao, Y. Wang, H. Wei, and W. Tong, "Photonic crystal fiber-based interferometric biosensor for streptavidin and biotin detection," IEEE J. Sel. Topics Quantum Electron., vol. 18, no. 4, pp. 1293–1297, Jul./Aug. 2012.
32. M. Deng, X. Sun, H. Wei, and J. Li, "Photonic crystal fiber-based modal interferometer for refractive index sensing," IEEE Photon. Technol. Lett., vol. 26, no. 6, pp. 531–534, Mar. 2014.
33. E. Coscelli, M. Sozzi, F. Poli, D. Passaro, A. Cucinotta, S. Selleri, R. Corradini, and R. Marchelli, "Toward a highly specific DNA biosensor: PNA-modified suspended-core photonic crystal fibers," IEEE J. Sel. Topics Quantum Electron., vol. 16, no. 4, pp. 967–972, Jul./Aug. 2010.
34. E. Haque, A. Al Noman, and F. Ahmed, "Numerical investigation of photonic crystal fiber-based biosensor for pathogens detection in water," IEEE Access, vol. 10, pp. 90013–90022, 2022.
35. N. Jahan, Md. M. Rahman, M. Ahsan, Md. A. Based, Md. M. Rana, S. Gurusamy, and J. Haider, "Photonic crystal fiber based biosensor for Pseudomonas bacteria detection: A simulation study," IEEE Access, vol. 9, pp. 42206–42215, 2021.
36. N. A. Mohammed et al., "Literature review: On-chip photonic crystals and photonic crystal fiber for biosensing and some novel trends," IEEE Access, vol. 10, pp. 47048–47065, 2022.
37. M. Stecher, C. Jansen, M. Ahmadi-Boroujeni, R. Lwin, A. Stefani, M. Koch, and G. E. Town, "Polymeric THz 2D photonic crystal filters fabricated by fiber drawing," IEEE Trans. Terahertz Sci. Technol., vol. 2, no. 2, pp. 203–211, Mar. 2012.
38. K. Ahmed, F. Ahmed, S. Roy, B. K. Paul, M. N. Aktar, D. Vigneswaran, and M. S. Islam, "Refractive index-based blood components sensing in terahertz spectrum," IEEE Sensors J., vol. 19, no. 9, pp. 3368–3375, May 2019.
39. D. Ouyang, S. Ruan, C. Guo, and H. Wei, "Low loss splicing between double-clad fiber and photonic crystal fiber using graded index fiber lens," J. Lightwave Technol., vol. 32, no. 14, pp. 2524–2529, Jul. 2014.
40. H. Wei, Y. Zhu, and S. Krishnaswamy, "Numerical analysis of waveguide coupling between photonic crystal fiber and single-mode fiber," IEEE Photon. Technol. Lett., vol. 27, no. 20, pp. 2142–2145, Oct. 2015.